Dalton Transactions

PAPER

View Article Online
View Journal

Cite this: DOI: 10.1039/c8dt02966k

Synthesis, gallium-68 radiolabelling and biological evaluation of a series of triarylphosphonium-functionalized DO3A chelators†

Adam J. Smith, [a,b] Peter J. Gawne, [a,b] Michelle T. Ma, [b] Philip J. Blower, [b] Richard Southworth *[b] and Nicholas J. Long *[a]

Radiolabelled lipophilic cations that accumulate in mitochondria according to the magnitude of the mitochondrial membrane potential can be used to report non-invasively on mitochondrial dysfunction in cardiovascular disease, cardiotoxicity, and cancer. While several such cations are already commercially available for SPECT imaging, PET offers greater promise in terms of sensitivity, resolution, and capacity for dynamic imaging and pharmacokinetic modelling. We have therefore synthesised a series of three triarylphosphonium-functionalised DO3A chelators for positron emitter gallium-68, with differing alkyl-functionalisation motifs to provide opportunities for tunable lipophilicity as a means of optimising their pharmacokinetics. To assess their capacity to report on mitochondrial membrane potential, we assessed their pharmacokinetic profiles in isolated tumour cells and isolated perfused rat hearts before and after mitochondrial depolarisation with the ionophore CCCP. All three compounds radiolabelled with over 97% RCY and exhibited log *D* values of between −3.12 and −1.81. *In vitro* assessment of the uptake of the radiotracers in cultured tumour cells showed a three-fold increase in uptake compared to unchelated [^{68}Ga]Ga(III). However, each complex exhibited less than 1% retention in healthy hearts, which was not significantly diminished by mitochondrial depolarisation with CCCP. This preliminary work suggests that while this approach is promising, the lipophilicity of this class of tracers must be increased in order for them to be useful as cardiac or cancer imaging agents.

Received 20th July 2018,
Accepted 3rd October 2018

DOI: 10.1039/c8dt02966k

rsc.li/dalton

Introduction

Lipophilic cations are widely used to map myocardial perfusion by means of SPECT, and to a lesser extent, PET imaging. They can accumulate in the mitochondrial matrix in a manner dependent on mitochondrial membrane potential ($\Delta\Psi_m$), which in normally functioning mitochondria is between 150–180 mV.[1–4] In lipophilic cations that have been successfully used as probes of $\Delta\Psi_m$, the charge is delocalised over a large molecular surface area and as such, the tracers can pass easily through the lipid bilayer membrane.[2] Application of the Nernst equation to monocations predicts 100- to 500-fold accumulation compared to the extracellular space, and at 37 °C, mitochondrial uptake of lipophilic cations increases 10-fold for every 61.5 mV increase in $\Delta\Psi_m$.[1,2] This means that the degree of uptake of lipophilic cations can be related to mitochondrial function or dysfunction; for example, compared to healthy mitochondria, $\Delta\Psi_m$ is reduced to below 100 mV in myocardial tissue recovering from reperfusion injury, and at least 60 mV higher in tumour cells, and the uptake of lipophilic cations varies accordingly.[5,6]

This basic concept has long been used experimentally to report on $\Delta\Psi_m$ through the use of fluorescent lipophilic cations such as tetramethylrhodamine (TMRE), BODIPY and Rhodamine-123.[7–9] These tracers show great utility in cell culture and isolated tissue preparations, however the poor depth penetration and lack of whole body scanning inherent to fluorescent tracers limits their overall utility. On the other hand, nuclear medicine imaging methodologies such as SPECT and PET provide unparalleled depth penetration, allowing whole body imaging; clinically, SPECT-based lipophilic cations such as [^{99m}Tc]Tc-sestaMIBI (Fig. 1) and [^{99m}Tc]Tc-tetrofosmin ($t_{\frac{1}{2}}$ = 6 h) are used.[10–13] A clinical PET "equivalent" to the SPECT radiopharmaceuticals [^{99m}Tc]Tc-sestaMIBI and [^{99m}Tc]Tc-tetrofosmin would enable higher resolution imaging, and potential detection of anatomically smaller

[a]Department of Chemistry, Imperial College London, Molecular Sciences Research Hub, White City Campus, 80 Wood Lane, W12 0BZ, UK. E-mail: n.long@imperial.ac.uk
[b]School of Biomedical Engineering and Imaging Sciences, King's College London, 4th Floor Lambeth Wing, St. Thomas' Hospital, London, SE1 7EH, UK. E-mail: richard.southworth@kcl.ac.uk

†Electronic supplementary information (ESI) available. See DOI: 10.1039/c8dt02966k

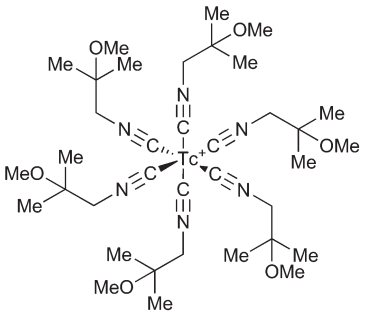

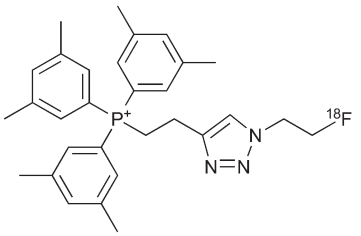

Fig. 1 [^{99m}Tc]Tc-sestaMIBI and [^{18}F]MitoPhos_07, two examples of lipophilic and cationic radiotracers.[10,27]

tissue defects with aberrant $\Delta\Psi_m$. In addition, PET radiotracers allow for dynamic imaging, so that the kinetics of influx and efflux can be easily followed. It should also be noted that there exist examples of multimodal optical/PET imaging agents, which consist of a fluorophore functionalised with a PET radioisotope.[14–16] These compounds allow for the combination of the high resolution of optical imaging with the depth penetration of PET imaging.

PET radioisotopes such as carbon-11 and fluorine-18 ($t_{\frac{1}{2}}$ = 20 and 109.7 min respectively) have previously been incorporated into lipophilic triphenylphosphonium (TPP) cations. TPP is widely known to target mitochondria since the cationic charge nominally residing on the phosphorus atom can be delocalised around the aromatic rings.[3,4,17,18] The first PET tracer to utilise TPP was designed by Fukuda *et al.* and consisted of TPP methylated with carbon-11 (methylTPP).[19] Since then, there have been many different types of TPP-functionalised PET tracers for mitochondrial imaging, most commonly using fluorine-18 since its longer half-life facilitates clinical imaging.[20–25] Recently, our group has synthesised the MitoPhos series of tracers, which are fluorine-18 radiolabelled alkyl-functionalised triarylphosphonium (TAP) cations, in order to provide radiotracers with tunable lipophilicity. One example of this series is [^{18}F]MitoPhos_07, shown in Fig. 1.[26,27]

Metallic PET radioisotopes, such as copper-64 and gallium-68 ($t_{\frac{1}{2}}$ = 12.7 h and 68 min respectively) have the advantage that once the chelator has been synthesised, the radiometal can be added *via* a simple final synthetic step. Chelators such as DO3A-xy-TPP, which consist of a DO3A chelating moiety, a xylyl linking group (xy) and a TPP cation, have been shown to chelate copper-64 to form effective tumour imaging agents.[28–30] Unlike cyclotron-produced copper-64, gallium-68 is generator-produced, and so has the potential to be more widely used as generators become clinically widespread.[31–34] There has been some preliminary work on synthesising gallium-labelled lipophilic cations for mitochondrial imaging *e.g.* Kardashinsky *et al.* have synthesised DO3A-xy-TAP chelators for gallium-67, in which the TAP groups exhibit methyl and pyridyl functionalisation.[35–37] However, no mitochondrial uptake studies have been performed on these chelators, and their utility as gallium-68 based imaging agents has yet to be explored.

In this study, we present a series of DO3A chelators for gallium-68 complexation, functionalised with triphenylphosphonium, tritolylphosphonium (TTP) and trixylylphosphonium (TXP) (Fig. 2). These chelators are designed to combine the rationale behind the DO3A-xy-TPP chelators previously used for copper-64 and gallium-67 chelation, with tunable lipophilicity afforded by alkyl-functionalised triarylphosphonium cations in order to form the novel chelators DO3A-xy-TTP and DO3A-xy-TXP.[27,29,37] After initial synthesis and characterisation of the ligands, their radiolabelling characteristics and log *D* values were analysed to give an indication of their potential use as mitochondrial imaging agents. The tracers

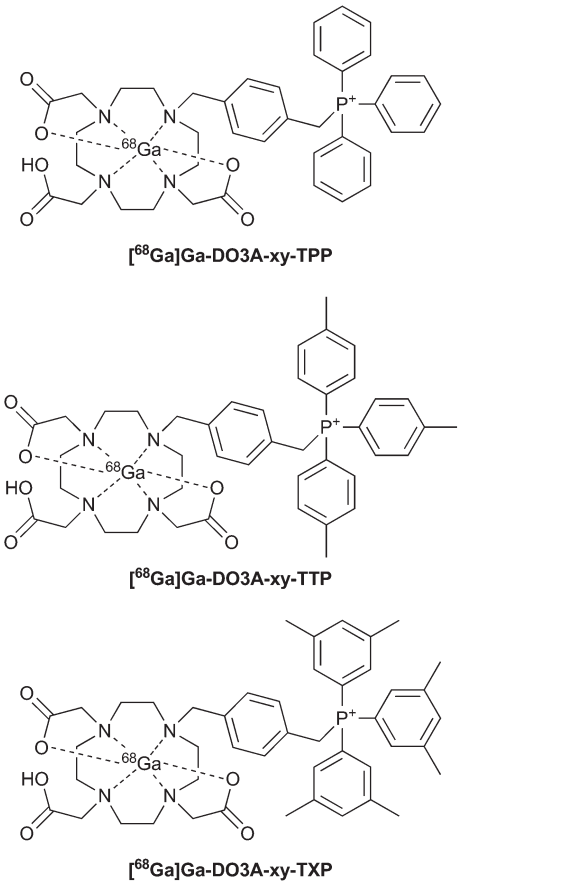

Fig. 2 The three gallium-68 chelate complexes synthesised in this study: [^{68}Ga]Ga-DO3A-xy-TPP, [^{68}Ga]Ga-DO3A-xy-TTP and [^{68}Ga]Ga-DO3A-xy-TXP.

were biologically evaluated in cultured tumour cells and using the *ex vivo* Langendorff isolated perfused heart model with a unique triple gamma detector system, which has been used previously in our group to assess radiotracer pharmacokinetics.[38–41]

Results

Synthesis of the DO3A-xy-TAP chelators

DO3A-xy-TAP chelators were synthesised as outlined in Scheme 1. The synthesis combined methodologies used by Haslop *et al.*, Wang *et al.* and Kardashinsky *et al.*[27,28,37] Firstly, an alkyl-functionalised aryl bromide was converted into a Grignard reagent before being reacted with phosphorus trichloride to form a triarylphosphine (**1**). This strategy allowed tuning of the final tracer lipophilicity by altering the alkyl functionalisation, in accordance with the work performed by Haslop *et al.*[27] Whilst anaerobic and anhydrous conditions were maintained as far as possible, some triarylphosphine was found by $^{31}P\{^{1}H\}$-NMR to be oxidised to its phosphine oxide. The phosphine oxide impurity did not require additional purification, since it was inert during the subsequent nucleophilic substitution step due to the lack of a phosphorus-centred lone pair.

Secondly, the triarylphosphine was reacted with α,α′-dibromo-*m*-xylene to form the phosphonium compound and incorporate the xylyl linking group (**2**). Wang *et al.* performed this reaction at 100 °C in toluene, forming a mixture of the desired monosubstituted product as well as starting material and disubstituted impurities.[28] Instead, we performed the reaction at the lowest temperature at which the dibromoxylene fully dissolves in toluene, *i.e.* 60 °C. At this temperature, as **2** forms, it precipitates out of the non-polar toluene solvent, and thus can be readily isolated by vacuum filtration.

The monocationic bromoxylene phosphonium derivative **2** was then reacted with tris-*tert*-butyl-protected DO3A hydrobromide to form TAP-functionalised DO3A derivatives (**3**).[42] Using sodium carbonate as an inorganic base allowed for the purification by recrystallisation of the tris-*tert*-butyl protected intermediate, as well as its characterisation by NMR. The final step was deprotection of the *tert*-butyl protected carboxylates (**3**) using trifluoroacetic acid, followed by purification by semipreparative reverse-phase HPLC.

Radiolabelling studies of DO3A-xy-TAP with $[^{68}Ga]GaCl_3$ eluate

All three DO3A-xy-TAP compounds were radiolabelled and analysed using the same protocol. The ligand was dissolved in aqueous ammonium acetate solution in order to partially neutralise the acidic generator eluate containing $[^{68}Ga]Ga(III)$. Next, the $[^{68}Ga]Ga(III)$ eluate was added, and the resulting mixture was heated at 100 °C for 30 minutes. As a quality control (QC) method, instant thin-layer chromatography (iTLC) was employed, using a mobile phase of 0.1 M EDTA, in which unchelated $[^{68}Ga]Ga(III)$ migrated to the solvent front, and left the cationic complex, which resisted transchelation to EDTA, on the baseline. iTLC analysis gave RCY values of 98, 100 and 97% for 100 μM concentrations of $[^{68}Ga]$Ga-DO3A-xy-TPP, TTP and TXP respectively. Due to the high RCY of the three radiolabelling processes, no post-purification was undertaken.

Finally, the reaction mixture was analysed by radioHPLC to determine whether a single complex had formed and to give an initial indication of its lipophilicity. The radioHPLC traces obtained for the three compounds are shown in normalised form in Fig. 3. In each trace, a small peak can be seen at approximately 2 minutes, which corresponds to unreacted/non-chelated $[^{68}Ga]Ga(III)$ species, and a single major peak corresponding to the complex, showing no evidence of isomerism. The relative retention times of the three compounds provide an insight into the lipophilicities of the three compounds. As can be seen from Fig. 2, increased TAP alkylation results in a longer retention time on a reverse-phase C-18 column, and indicates relatively greater lipophilicity. This trend is also seen in analogous HPLC traces of the unchelated

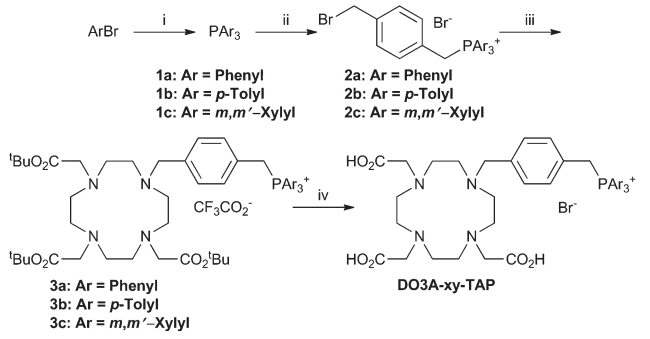

Scheme 1 Synthesis of DO3A-xy-TAP chelators. DO3A tris-^{t}Bu·HBr was synthesised according to previously reported procedures.[42] Reaction conditions: (i) Mg then PCl_3, dry THF, anaerobic conditions; (ii) α,α′-dibromo-*p*-xylene, toluene, 60 °C; (iii) DO3A tris-^{t}Bu·HBr, Na_2CO_3, MeCN, reflux; (iv) TFA, semi-prep HPLC. The choice of the aryl bromide determines which DO3A-xy-TAP variant is synthesised: Ar = phenyl, DO3A-xy-TPP; Ar = tolyl, DO3A-xy-TTP; Ar = *m*-xylyl, DO3A-xy-TXP.

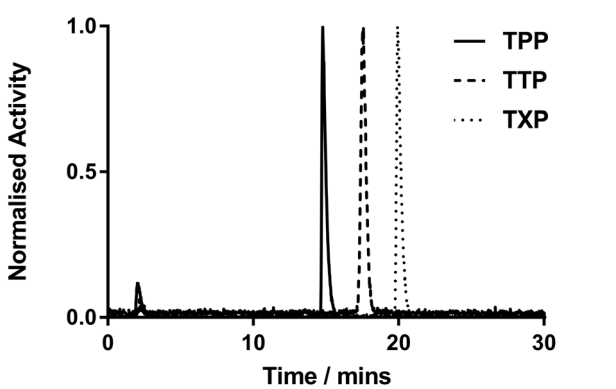

Fig. 3 RadioHPLC traces of the three labelled $[^{68}Ga]$Ga-DO3A-xy-TAP compounds (eluent gradient: 100% A for 5 min; 0–80% B in A for 20 min; 100% A for 5 min; flow rate 1 mL min^{-1}). All traces have been normalised such that the maximum activity measured for each compound is equal to 1.

Table 1 Retention times (in minutes) of the unchelated DO3A-xy-TAP ligands, along with their gallium-68-radiolabelled analogues as measured by HPLC. HPLC conditions are identical to those described in Fig. 3

Ar=	Unchelated ligand	[^{68}Ga]Ga complex
TPP	14.3	14.8
TTP	17.2	17.6
TXP	18.5	19.9

ligands; the retention times of which are summarised in Table 1. The unchelated ligands also show shorter HPLC retention times by HPLC than their gallium-68-labelled counterparts, which indicates an increase in lipophilicity upon chelation, a result of the hydrophilicity of the carboxylate arms decreasing upon binding to the metal centre.

Lipophilicity measurements of [^{68}Ga]Ga-DO3A-xy-TAP compounds

To measure the lipophilicities of the radiotracers, their octanol/PBS partition coefficients at pH 7.4 ($\log D$) were determined using a conventional 'shake-flask' method. The $\log D$ values, shown in Fig. 4, were determined to be −3.12 ± 0.17, −2.66 ± 0.09 and −1.81 ± 0.02 for [^{68}Ga]Ga-DO3A-xy-TPP, TTP and TXP respectively (n = 6 for all compounds).

In vitro quantification of [^{68}Ga]Ga-DO3A-xy-TXP uptake in tumour cells

Intracellular/extracellular concentration ratios for [^{68}Ga]Ga-DO3A-xy-TXP and unchelated [^{68}Ga]Ga(III) in breast cancer cells (MDA-MB 231) *in vitro* were calculated, and are summarised in Fig. 5. [^{68}Ga]Ga-DO3A-xy-TXP shows a ratio of 10.03 ± 0.45, indicating that the tracers localise inside the tumour cells. In comparison, [^{68}Ga]Ga(III) shows a ratio of 3.43 ± 0.39, indicating that the chelator facilitates a three-fold increase in radiotracer uptake compared to unchelated [^{68}Ga]Ga(III). A trypan blue cell viability study showed over 90% of cells used in both the [^{68}Ga]Ga-DO3A-xy-TXP and control experiments survived.

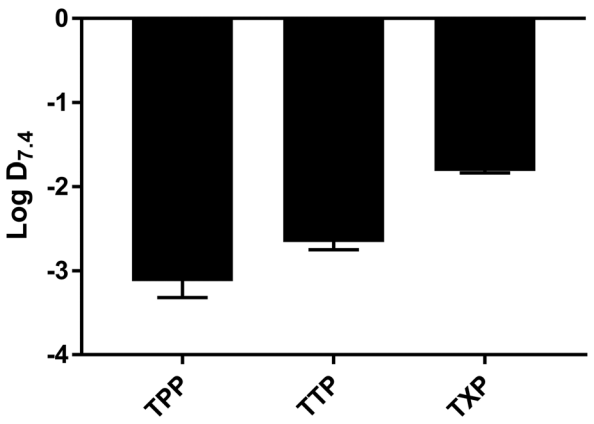

Fig. 4 Log D values obtained of the three labelled [^{68}Ga]Ga-DO3A-xy-TAP compounds. Data are mean ± SD (n = 6).

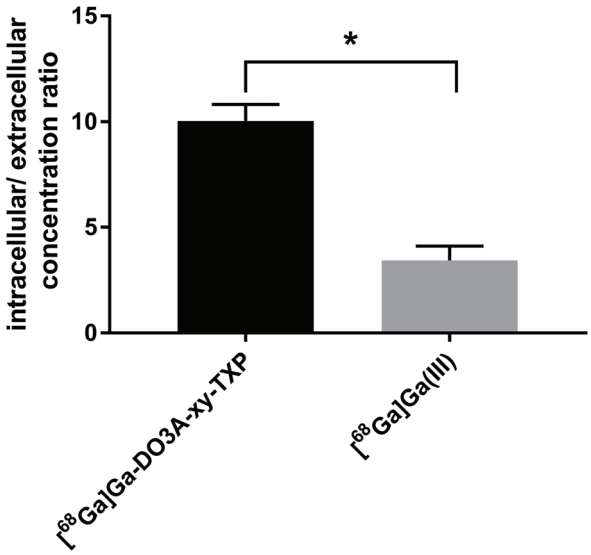

Fig. 5 Results of the *in vitro* tumour cell uptake experiment for [^{68}Ga]Ga-DO3A-xy-TXP and unchelated [^{68}Ga]Ga(III) control. Measurements were taken in triplicate. Data are mean ± SD. * = P < 0.05.

Quantification of [^{68}Ga]Ga-DO3A-xy-TXP myocardial uptake using the Langendorff isolated perfused heart model

We have previously made use of the Langendorff isolated perfused heart model to provide an *ex vivo* assessment of myocardial radiotracer uptake, with a unique triple radiodetector system which allows for accurate determination of time-activity curves.[38–41] The time-activity curves for each of the three radiodetectors quantify radiotracer entering the heart (arterial detector), radiotracer retention in the heart (heart detector) and radiotracer exiting the heart (venous detector). The *ex vivo* nature of the experiment means that the behaviour of the tracer in the myocardium can be evaluated accurately and reproducibly without the complications of the *in vivo* setting such as aberrant metabolism or regional changes in perfusion, and haemodynamic parameters can be easily monitored, whilst maintaining constant perfusion to determine the specific contribution of mitochondrial membrane potential to tracer pharmacokinetics.

To assess radiotracer uptake under conditions in which $\Delta\Psi_m$ is reduced, the heart was infused with a 600 nM solution of the ionophore carbonyl cyanide *m*-chlorophenyl hydrazone (CCCP).[43] We have previously found that this concentration is optimal to effect complete $\Delta\Psi_m$ depolarisation, validated using the clinical SPECT radiopharmaceutical, [^{99m}Tc]Tc-sestaMIBI (Fig. 1) to ensure validity of the model for this set of experiments.[44] As shown in Fig. 6A and summarised in Fig. 6B, [^{99m}Tc]Tc-sestaMIBI demonstrates 30 ± 0.03% (n = 4) radiotracer retention after 15 minutes in hearts under normal conditions, but 0 ± 0.04% (n = 4) retention after 15 minutes in hearts under depolarising conditions.[12]

[^{68}Ga]Ga-DO3A-xy-TXP (1 MBq) was injected as a bolus into the flow of Krebs buffer. Arterial influx, myocardial retention and venous efflux of radiotracer were measured using each

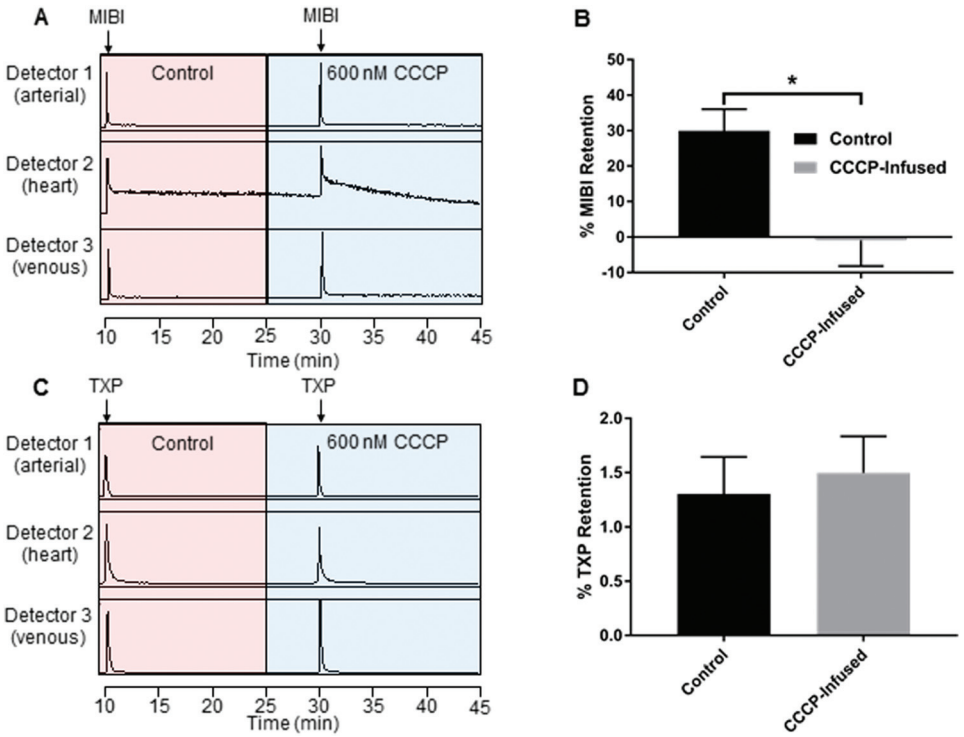

Fig. 6 (A and C) Representative example of data output of the triple-gamma detector system for [^{99m}Tc]Tc-sestaMIBI and [^{68}Ga]Ga-DO3A-xy-TXP respectively. (B and D) Retention values obtained using the two-injection protocol 15 minutes post-injection for [^{99m}Tc]Tc-sestaMIBI and [^{68}Ga]Ga-DO3A-xy-TXP respectively. Control data were obtained from the injection before CCCP infusion, whilst CCCP data were obtained during 600 nM CCCP infusion. Data for [^{99m}Tc]Tc-sestaMIBI are mean ± SD (n = 4). * = P < 0.05. Data for [^{68}Ga]Ga-DO3A-xy-TXP are mean ± SD (n = 3).

respective γ-detector (Fig. 6A and C) for 15 min. Then, to assess radiotracer uptake under depolarising conditions, the same heart was infused with CCCP. After 5 min of infusion with CCCP, the second bolus of [^{68}Ga]Ga-DO3A-xy-TXP was injected, and the passage of radioactivity through the perfusion system was monitored using the three γ-detectors. As shown by Fig. 6C, most of the injected [^{68}Ga]Ga-DO3A-xy-TXP washed out of the heart within 3 minutes of bolus administration, irrespective of whether the mitochondria were depolarised. This stands in contrast to the control data for mitochondrial depolarisation dependant uptake of [^{99m}Tc]Tc-sestaMIBI discussed previously. The average retained gallium-68 activity between 14–15 minutes post-injection over 3 experiments is reported in Fig. 6D. [^{68}Ga]Ga-DO3A-xy-TXP showed 1% retention in both control and CCCP-infused hearts. Over 3 experiments, there was no statistically significant difference between [^{68}Ga]Ga-DO3A-xy-TXP retention in control and CCCP infused hearts.

Discussion

The series of DO3A-xy-TAP compounds was designed to be simple to synthesise and purify, whilst also being easy to modify in order to generate a series of compounds with tunable lipophilicity. Unlike other syntheses of TAP-functionalised DO3A compounds, this work utilises a highly modular approach, which allows a library of compounds to be synthesised using identical reaction protocols. Use of a lower reaction temperature during formation of the phosphonium cation allows for the facile isolation of the pure target compound, which is especially useful given the difficulties in purifying phosphonium cations using column chromatography.

Upon radiolabelling, the three gallium-68 radiolabelled compounds synthesised all show high RCY values above 97%, despite the size mismatch between DO3A and Ga(III) cations. Whilst DO3A is not an ideal chelator for Ga(III) cations since radiolabelling requires heating and lengthy reaction times, it was chosen for the simplicity of its functionalisation chemistry. A useful part of this work is the method for the QC of gallium-68 labelled lipophilic cations. Basing this method on the facile chelation of Ga(III) by EDTA means that this method should be easily applicable to future syntheses of all gallium-68 labelled lipophilic cations.

Functionalisation of the TAP moiety with alkyl groups has been shown to dramatically affect the lipophilicity of the radiotracers with a 0.5 unit difference between the TPP and TTP-functionalised compounds, and a 0.8 unit difference between the TTP and TXP-functionalised compounds. It is interesting that even when conjugated to the bulky and hydrophilic DO3A chelator, such a small change as the addition of three methyl groups to the TPP group has such a dramatic effect on the log D values. The log D values of the compounds are low when compared to other lipophilic cationic compounds such as

[^{99m}Tc]Tc-sestaMIBI, which has a log D value of 1.29.[45] Nevertheless, it was decided to assess the tracer *ex vivo* as there is precedent of cations with low log D values crossing lipid bilayer membranes.[25,46]

Uptake experiments with [^{68}Ga]Ga-DO3A-xy-TXP in tumour cells were undertaken *in vitro*, due to the high $\Delta\Psi_m$ values often found in tumour cells.[1,2,6,47–49] In this study, [^{68}Ga]Ga-DO3A-xy-TXP showed a three-fold increase in uptake in the cancer cell line when compared to unchelated [^{68}Ga]Ga(III), indicating that the chelator facilitates uptake of gallium-68 into tumour cells.

Analysis using the perfused heart model showed no statistically significant difference in [^{68}Ga]Ga-DO3A-xy-TXP retention between healthy and CCCP-infused hearts. In addition, the cardiac uptake of our compounds was low when compared to the parallel study performed using [^{99m}Tc]Tc-sestaMIBI. This is likely a result of the lower lipophilicity of [^{68}Ga]Ga-DO3A-xy-TXP hindering passage through the lipid bilayer membrane. Since the membrane potential in a normally functioning heart does not facilitate uptake of these tracers in cardiac cells, there will then be no difference in uptake once the mitochondria have been depolarized by CCCP infusion. This preliminary work suggests that while this approach is promising from a synthetic strategy perspective, the lipophilicity of this class of tracers must be increased in order for them to be useful as cardiac or cancer imaging agents.

Conclusions

We have synthesised a series of TAP-functionalised DO3A ligands for gallium-68 chelation with a view to synthesising lipophilic cationic radiotracers. The synthetic methodology developed is effective and entirely modular, and can be the basis of a strategy for synthesising libraries of tracers with tunable lipophilicities, by varying the chelator, linker and cation. The results encourage the development of future gallium-68 labelled lipophilic cations with chelators more appropriate for the efficient formation of lipophilic and positively charged complexes of gallium-68.

Experimental procedures

Materials and instrumentation

Commercially available reagent grade solvents and chemicals were used without further purification. All gas mixtures were purchased from BOC Industrial Gases. ^{1}H, ^{13}C{^{1}H}, ^{19}F{^{1}H}, ^{31}P{^{1}H}, COSY, HSQC, and HMBC NMR spectra were obtained using a Bruker AVIII 400 spectrometer. High Resolution Electrospray Mass Spectrometry was carried out on a Waters LCT Premier (ES-ToF)/Acquity i-Class spectrometer. HPLC was performed on an Agilent 1200 Series Liquid Chromatograph with UV and LabLogic Flow-Count detector with a sodium-iodide probe (B-FC-3200). Mobile phase A contained water with 0.1% TFA, and mobile phase B contained MeCN with 0.1% TFA. Semi-preparative reverse phase HPLC was conducted using an Agilent Eclipse XDB-C18 column (21.2 × 150 mm, 5 μm) with a 5 mL min^{-1} flow rate and UV spectroscopic detection at 214 nm. Analytical reverse phase HPLC was conducted using an Agilent Eclipse XDB-C18 column (4.6 × 150 mm, 5 μm) with a 1 mL min^{-1} flow rate and UV spectroscopic detection at 250 nm. Gallium-68 was eluted as [^{68}Ga]$GaCl_3$ from an Eckert and Ziegler gallium-68 generator using a 0.1 M solution of hydrochloric acid.

Synthesis

Synthesis of tris(3,5-dimethylphenyl)phosphane (**1c**) was performed according to previously reported literature procedures by Haslop *et al.*[27] Synthesis of 1,4,7-tris(*tert*-butoxycarbonylmethyl)-1,4,7,10-tetraazacyclododecane hydrobromide (DO3Atriester·HBr) was performed according to previously reported literature procedures by Jagadish *et al.*[42]

Tri-*p*-tolylphosphane (1b). This compound was originally synthesised by Mann *et al.*[50] The methodology used here was a modification of the procedure described by Haslop *et al.*[27] A solution of 4-bromotoluene (2.89 mL, 23.5 mmol) in anhydrous THF (10 mL) was added dropwise whilst maintaining reflux to magnesium turnings (0.57 g, 23.5 mmol) in a Schlenk flask under N_2. The resulting suspension was stirred for 2 h before a solution of PCl_3 (0.69 mL, 7.8 mmol) in anhydrous THF (15 mL) was added dropwise whilst maintaining reflux, and the resulting mixture was stirred for a further 2 h. The reaction was quenched with water (10 mL), and the organic phase was isolated. The organic solvent was removed under reduced pressure to yield the title compound as a pale yellow solid (0.96 g, 40%). ^{1}H-NMR (400 MHz, $CDCl_3$) δ_H (ppm): 7.24 (6H, m), 7.17 (6H, m), 2.38 (9H, s, C$\underline{H}_3$). ^{13}C{^{1}H}-NMR (100 MHz, $CDCl_3$) δ_c (ppm): 138.6, 133.8, 129.4, 129.3, 21.4. ^{31}P{^{1}H}-NMR (162 MHz, $CDCl_3$) δ_P (ppm): −7.9. HRMS (ES-TOF+): m/z calcd for $C_{21}H_{22}P$ ([M + H]$^+$) 305.1459, found 305.1445.

General procedure 1: monosubstitution of α,α′-dibromo-*p*-xylene with aryl-functionalized triarylphosphines (2)

The methodology used was a modification of the procedure described by Wang *et al.*[28] α,α′-Dibromo-*p*-xylene (1 eq.) was added to toluene (5 mL) and heated to 60 °C until all the solid had dissolved. To this, a solution of the triarylphosphine (1 eq.) in toluene (6 mL) was added dropwise, before the resulting solution was stirred at 60 °C under an N_2 atmosphere overnight. The white precipitate was isolated by filtration, before being washed with toluene (5 mL) and Et_2O (2 × 10 mL), then dried *in vacuo* to yield the desired product.

(4-(Bromomethyl)benzyl)triphenylphosphonium bromide (2a). This compound was originally synthesised by Wang *et al.*[28] Following **general procedure 1**, the title compound was prepared from α,α′-dibromo-*p*-xylene (0.53 g, 2 mmol) and triphenylphosphine (0.54 g, 2 mmol) as a white solid (0.86 g, 82%). ^{1}H NMR (400 MHz, $CDCl_3$) δ_H (ppm): 7.73 (9H, m, *m*/*p*-Ar), 7.60 (6H, m, *o*-Ar), 7.11 (4H, d, $^{3}J_{HH}$ = 1.3 Hz, $C_6\underline{H}_4$), 5.50 (2H, d, $^{2}J_{HP}$ = 14.6 Hz, C$\underline{H}_2$P), 4.37 (2H, d, $^{4}J_{HH}$ = 1.3 Hz,

CH_2Br). $^{13}C\{^1H\}$-NMR (100 MHz, $CDCl_3$) δ_C (ppm): 138.2 (d, $^4J_{CP}$ = 4.4 Hz, *p*-Ar), 135.1 (d, $^5J_{CP}$ = 2.8 Hz), 134.5 (d, $^2J_{CP}$ = 9.3 Hz, *o*-Ar), 132.1 (d, $^3J_{CP}$ = 6.1 Hz, C_6H_4), 130.3 (d, $^3J_{CP}$ = 6.1 Hz, *m*-Ar), 129.5 (d, $^4J_{CP}$ = 3.5 Hz, C_6H_4), 127.9 (d, $^3J_{CP}$ = 8.8 Hz), 117.9 (d, $^1J_{CP}$ = 85.9 Hz, *i*-Ar), 33.0 (CH_2Br), 30.5 (d, $^1J_{CP}$ = 47.2 Hz, CH_2P). $^{31}P\{^1H\}$-NMR (162 MHz, $CDCl_3$) δ_P (ppm): 23.5. HRMS (ES-TOF+): *m*/*z* calcd for $C_{26}H_{23}BrP$ ($[M - Br]^+$) 445.0721, found 445.0737.

(4-(Bromomethyl)benzyl)tri-*p*-tolylphosphonium bromide (2b). Following **general procedure 1**, the title compound was prepared from α,α′-dibromo-*p*-xylene (0.53 g, 2 mmol) and tri-*p*-tolylphosphane (0.72 g, 2 mmol) as a white solid (1.04 g, 92%). ^1H NMR (400 MHz, $CDCl_3$) δ_H (ppm): 7.54 (6H, m, *m*-Ar), 7.38 (6H, dd, $^3J_{HP}$ = 8.2, $^3J_{HH}$ = 3.2 Hz, *o*-Ar), 7.13 (2H, d, $^3J_{HH}$ = 8.1 Hz, C_6H_4), 7.08 (2H, dd, $^3J_{HH}$ = 8.4, $^4J_{HP}$ = 2.4 Hz, C_6H_4), 5.24 (2H, d, $^2J_{HP}$ = 14.5 Hz, CH_2P), 4.38 (2H, s, CH_2Br), 2.44 (9H, s, CH_3). $^{13}C\{^1H\}$-NMR (100 MHz, $CDCl_3$) δ_C (ppm): 146.3 (d, $^5J_{CP}$ = 2.6, Hz, C_6H_4), 138.1 (d, $^4J_{CP}$ = 3.9 Hz, *o*-Ar), 134.3 (d, $^2J_{CP}$ = 10.4 Hz, *p*-Ar), 132.0 (d, $^3J_{CP}$ = 5.7 Hz, C_6H_4), 130.4 (d, $^3J_{CP}$ = 3.4 Hz, *m*-Ar), 129.5 (d, $^4J_{CP}$ = 3.6 Hz, C_6H_4), 128.1 (d, $^2J_{CP}$ = 8.6 Hz, C_6H_4), 114.6 (d, $^1J_{CP}$ = 88.7 Hz, *i*-Ar), 33.1 (CH_2Br), 30.9 (d, $^1J_{CP}$ = 48.1 Hz, CH_2P), 22.0 (CH_3). $^{31}P\{^1H\}$-NMR (162 MHz, $CDCl_3$) δ_P (ppm): 22.4. HRMS (ES-TOF+): *m*/*z* calcd for $C_{29}H_{29}BrP$ ($[M - Br]^+$) 529.1660, found 529.1669. Anal. calcd for $C_{29}H_{29}PBr_2$ (found): C, 61.29 (61.22); H 5.14 (5.26).

(4-(Bromomethyl)benzyl)tris(3,5-dimethylphenyl)phosphonium bromide (2c). Following **general procedure 1**, the title compound was prepared from α,α′-dibromo-*p*-xylene (0.53 g, 2 mmol) and tris(3,5-dimethylphenyl)phosphane (0.87 g, 2 mmol) as a white solid (2.74 g, 88%). ^1H NMR (400 MHz, $CDCl_3$) δ_H (ppm): 7.34 (3H, s, *p*-Ar), 7.21 (6H, d, $^3J_{HP}$ = 13.0 Hz, *o*-Ar), 7.15 (2H, d, $^3J_{HH}$ = 7.6 Hz, C_6H_4), 7.02 (2H, dd, $^3J_{HH}$ = 8.0, $^4J_{HP}$ = 2.7 Hz, C_6H_4), 5.21 (2H, d, $^2J_{HP}$ = 14.3 Hz, CH_2P), 4.40 (2H, s, CH_2Br), 2.36 (18H, s, CH_3). $^{13}C\{^1H\}$-NMR (100 MHz, $CDCl_3$) δ_C (ppm): 140.3 (d, $^2J_{CP}$ = 12.3 Hz, C_6H_4), 138.0 (d, $^5J_{CP}$ = 3.5 Hz, C_6H_4), 136.8 (d, $^4J_{CP}$ = 3.5 Hz, C_6H_4), 132.1 (d, $^3J_{CP}$ = 5.1 Hz, C_6H_4), 131.7 (d, $^2J_{CP}$ = 10.1 Hz, *o*-Ar), 129.3 (d, $^4J_{CP}$ = 3.5 Hz, *p*-Ar), 128.5 (d, $^3J_{CP}$ = 8.7 Hz, *m*-Ar), 117.8 (d, $^1J_{CP}$ = 84.5 Hz, *i*-Ar), 33.1 (CH_2Br), 30.9 (d, $^1J_{CP}$ = 46.6 Hz, CH_2P), 21.5 (CH_3). $^{31}P\{^1H\}$-NMR (162 MHz, $CDCl_3$) δ_P (ppm): 22.7. HRMS (ES-TOF+): *m*/*z* calcd for $C_{32}H_{35}BrP$ ($[M - Br]^+$) 529.1660, found 529.1643. Anal. calcd for $C_{32}H_{35}PBr_2$ (found): C, 62.97 (62.98); H, 5.78 (5.73).

General procedure 2 – coupling of triarylphosphane-substituted bromoxylene to DO3Atriester hydrobromide (3)

The methodology was a modification of the procedure described by Kardashinsky *et al.*[37] To a solution of DO3Atriester·HBr (1 eq.) and triarylphosphane-substituted bromoxylene (1 eq.) in MeCN (15 mL), Na_2CO_3 (5 eq.) was added, and the resulting suspension was heated to reflux and stirred under an N_2 atmosphere overnight. The inorganic base was removed by filtration and the solvent removed under reduced pressure. The resulting residue was recrystallized from acetone/Et_2O to yield the desired product.

Triphenyl(4-((4,7,10-tris(2-(*tert*-butoxy)-2-oxoethyl)-1,4,7,10-tetraazacyclododecan-1-yl)methyl)benzyl)phosphonium bromide (3a). Following **general procedure 2**, the title compound was prepared from DO3Atriester·HBr (0.30 g, 0.5 mmol), **2a** (0.26 g, 0.5 mmol) and Na_2CO_3 (0.26 g, 2.5 mmol) as a white solid (0.37 g, 76%). ^1H NMR (400 MHz, $CDCl_3$) δ_H (ppm): 7.78 (3H, tt, $^3J_{HH}$ = 6.9, $^4J_{HH}$ = 1.7 Hz, *p*-Ar), 7.74–7.63 (12H, m, *o*/*m*-Ar), 7.05–7.04 (4H, m, C_6H_4), 5.33 (2H, broad s, CH_2P), 3.64 (2H, s, $C_6H_4CH_2$), 3.41–2.11 (22H, m, macrocycle H/CH_3CO_2), 1.47 (18H, s, *cis*-$C(CH_3)_3$), 1.43 (9H, s, *trans*-$C(CH_3)_3$). $^{13}C\{^1H\}$-NMR (100 MHz, $CDCl_3$) δ_C (ppm): 173.7 (C=O), 172.7 (C=O), 135.6 (d, $^5J_{CP}$ = 4.0 Hz), 135.3 (d, $^4J_{CP}$ = 2.7 Hz), 134.4 (d, $^3J_{CP}$ = 9.8 Hz), 131.6 (d, $^3J_{CP}$ = 5.3 Hz), 130.9 (d, $^4J_{CP}$ = 1.8 Hz), 130.4 (d, $^2J_{CP}$ = 12.8 Hz), 129.9 (d, $^2J_{CP}$ = 8.7 Hz), 117.1 (d, $^1J_{CP}$ = 86.0 Hz), 83.1 (*cis*-$C(CH_3)_3$), 82.6 (*trans*-$C(CH_3)_3$), 57.9, 57.0, 50.9, 30.8 (d, $^1J_{CP}$ = 46.5 Hz, CH_2P), 28.2 ($C(CH_3)_3$), 28.0 ($C(CH_3)_3$). $^{31}P\{^1H\}$-NMR (162 MHz, $CDCl_3$) δ_P (ppm): 23.1. HRMS (ES-TOF+): *m*/*z* calcd for $C_{52}H_{72}N_4O_6P$ ($[M - Br]^+$) 879.5190, $C_{52}H_{73}N_4O_6P$ ($[M - Br + H]^{2+}$) 440.2628, $C_{52}H_{74}N_4O_6P$ ($[M - Br + 2H]^{3+}$) 293.8443. Found: 879.5258, 440.2600, 293.8420.

Tri-*p*-tolyl(4-((4,7,10-tris(2-(*tert*-butoxy)-2-oxoethyl)-1,4,7,10-tetraazacyclododecan-1-yl)methyl)benzyl)phosphonium bromide (3b). Following **general procedure 2**, the title compound was prepared from DO3Atriester·HBr (0.30 g, 0.5 mmol), **2b** (0.28 g, 0.5 mmol) and Na_2CO_3 (0.26 g, 2.5 mmol) as a white solid (0.23 g, 47%). ^1H NMR (400 MHz, $CDCl_3$) δ_H (ppm): 7.57–7.52 (6H, m, *o*-Ar), 7.43 (6H, dd, $^3J_{HH}$ = 8.3, $^4J_{HH}$ = 3.3 Hz, *m*-Ar), 7.07 (2H, dd, $^3J_{HH}$ = 8.3, $^4J_{HH}$ = 2.3 Hz, C_6H_4), 7.03 (2H, d, $^3J_{HH}$ = 8.1 Hz, C_6H_4), 5.18 (2H, d, $^2J_{HP}$ = 14.4 Hz, CH_2P), 3.68 (2H, s, $C_6H_4CH_2$), 3.43–2.18 (16H, m, macrocycle H) 3.04–3.00 (6H, m, CH_2CO_2), 2.47 (9H, s, $ArCH_3$) 1.48 (18H, s, *cis*-$C(CH_3)_3$), 1.43 (9H, s, *trans*-$C(CH_3)_3$). $^{13}C\{^1H\}$-NMR (100 MHz, $CDCl_3$) δ_C (ppm): 173.7 (C=O), 172.7 (C=O), 146.4 (C_6H_4), 135.6 (C_6H_4), 134.3 (d, $^2J_{CP}$ = 10.3 Hz, *o*-Ar), 131.5 (d, $^4J_{CP}$ = 6.4 Hz, C_6H_4), 131.0 (d, $^3J_{CP}$ = 12.5 Hz, C_6H_4), 130.8 (*m*-Ar), 127.2 (d, $^4J_{CP}$ = 8.5 Hz, *p*-Ar), 114.6 (d, $^1J_{CP}$ = 88.7 Hz, *i*-Ar), 83.0 ($C(CH_3)_3$), 82.6 ($C(CH_3)_3$), 58.0 ($C_6H_4CH_2$), 56.9 (CH_2CO_2), 56.0 (CH_2CO_2), 51.0 (broad, macrocycle C), 49.4 (broad, macrocycle C), 31.1 (d, $^1J_{CP}$, CH_2P), 28.2 (*cis*-$C(CH_3)_3$), 28.0 (*trans*-$C(CH_3)_3$), 22.0 (Ar-CH_3). $^{31}P\{^1H\}$-NMR (162 MHz, $CDCl_3$) δ_P (ppm): 22.1. HRMS (ES-TOF+): *m*/*z* calcd for $C_{55}H_{78}N_4O_6P$ ($[M - Br]^+$) 921.5659, $C_{55}H_{79}N_4O_6P$ ($[M - Br + H]^{2+}$) 461.2863. Found: 921.5684, 461.2828.

Tris(3,5-dimethylphenyl)(4-((4,7,10-tris(2-(*tert*-butoxy)-2-oxoethyl)-1,4,7,10-tetraazacyclododecan-1-yl)methyl)benzyl)phosphonium bromide (3c). Following **general procedure 2**, the title compound was prepared from DO3Atriester·HBr (0.30 g, 0.5 mmol), **2c** (0.31 g, 0.5 mmol) and Na_2CO_3 (0.26 g, 2.5 mmol) as a white solid (0.36 g, 70%). ^1H NMR (400 MHz, $CDCl_3$) δ_H (ppm): 7.35 (3H, s, *p*-Ar), 7.21 (6H, d, $^3J_{HP}$ = 13.1 Hz, *o*-Ar), 7.11 (2H, d, $^3J_{HH}$ = 8.0 Hz), 7.05 (2H, dd, $^3J_{HH}$ = 8.2, $^4J_{HP}$ = 2.4 Hz), 5.15 (2H, d, $^2J_{HP}$ = 14.2 Hz, CH_2P), 3.68 (2H, s), 3.05 (2H, s), 3.01 (4H, s), 2.97–2.16 (16H, m, macrocycle H), 2.36 (18H, s, Ar–CH_3), 1.48 (18H, s, *cis*-$C(CH_3)_3$), 1.44 (9H, s, *trans*-$C(CH_3)_3$). $^{13}C\{^1H\}$-NMR (100 MHz, $CDCl_3$) δ_C (ppm): 173.6 (C=O), 172.7 (C=O), 140.2 (d, $^2J_{CP}$ = 12.6 Hz, C_6H_4),

136.8 (*p*-Ar), 135.9 ($\underline{C}_6H_4$), 131.6 (*o*-Ar), 131.5 ($\underline{C}_6H_4$), 130.7 ($\underline{C}_6H_4$), 127.5 (d, $^3J_{CP}$ = 8.3 Hz, *m*-Ar), 117.7 (d, $^1J_{CP}$ = 84.9 Hz, *i*-Ar), 82.9 ($\underline{C}H_2CO_2$), 82.5 ($\underline{C}H_2CO_2$), 57.9 ($C_6H_4\underline{C}H_2$), 56.7 ($\underline{C}H_2CO_2$), 55.9 ($\underline{C}H_2CO_2$), 50.8 (broad, macrocycle $\underline{C}$), 49.2 (broad, macrocycle $\underline{C}$), 30.9 (d, $^1J_{CP}$ = 48.5 Hz, $\underline{C}H_2P$), 28.1 (*cis*-$C(\underline{C}H_3)_3$), 27.9 (*trans*-$C(\underline{C}H_3)_3$), 21.5 (Ar-$\underline{C}H_3$). $^{31}P\{^1H\}$-NMR (162 MHz, $CDCl_3$) δ_P (ppm): 22.4. HRMS (ES-TOF+): *m*/*z* calcd for $C_{58}H_{84}N_4O_6P$ ($[M - Br]^+$) 963.6129, $C_{58}H_{85}N_4O_6P$ ($[M - Br + H]^{2+}$) 482.3098. Found: 963.6139, 482.2990.

General procedure 3 – deprotection of *tert*-butyl protected DO3A-xy-TAP compounds using trifluoroacetic acid (4)

The methodology was a modification of the procedure described by Kardashinsky *et al.*[37] *tert*-butyl protected compounds were dissolved in trifluoroacetic acid (reaction mixture concentration 0.1 g mL^{-1}) and stirred at rt under an N_2 atmosphere for 24 h. The acid was removed *in vacuo*, before the residue was taken up in H_2O (50 mL) and washed with $CHCl_3$ (3 × 10 mL). The aqueous solvent was removed under reduced pressure, before the residue was purified *via* semi-preparative HPLC methods.

DO3A-xy-TPP trifluoroacetate. Following **general procedure 3**, the title compound was prepared from **3a** (0.25 g, 0.26 mmol) and trifluoroacetic acid (2.5 mL) as a white solid (0.16 g, 73%). ^{1}H NMR (400 MHz, MeOD) δ_H (ppm): 7.91 (3H, td, $^3J_{HH}$ = 7.3, $^4J_{HH}$ = 1.8 Hz, *p*-Ar), 7.78–7.62 (12H, m, *o*,*m*-Ar), 7.51 (2H, d, $^3J_{HH}$ = 7.8 Hz, $C_6\underline{H}_4$), 7.08 (2H, dd, $^3J_{HH}$ = 8.0, $^4J_{HP}$ = 2.7 Hz, $C_6\underline{H}_4$), 4.95 (2H, d, $^2J_{HP}$ = 15.1 Hz, $C\underline{H}_2P$), 4.34 (2H, s), 3.97 (2H, s), 3.64 (2H, s), 3.39 (4H, s), 3.29–3.02 (16H, m). $^{13}C\{^1H\}$-NMR (100 MHz, MeOD) δ_C (ppm): 162.8 ($\underline{C}$═O), 162.5 ($\underline{C}$═O), 136.6 (*p*-Ar), 135.3 ($^3J_{CP}$ = 9.1 Hz, *m*-Ar), 133.2 ($^3J_{CP}$ = 5.2 Hz, $\underline{C}_6H_4$), 131.5 ($^2J_{CP}$ = 13.6 Hz, *o*-Ar), 119.6 ($\underline{C}_6H_4$), 119.0 ($^1J_{CP}$ = 86.9 Hz, *i*-Ar), 116.7 ($\underline{C}_6H_4$), 58.5, 55.6, 54.1, 50.5 (broad s), 50.4 (broad s), 30.3 ($^1J_{CP}$ = 48.6 Hz, $\underline{C}H_2P$). $^{19}F\{^1H\}$-NMR (377 MHz, MeOD) δ_F (ppm): −73.0. $^{31}P\{^1H\}$-NMR (162 MHz, MeOD) δ_P (ppm): 26.8. HRMS (ES-TOF+): *m*/*z* calcd for $C_{40}H_{48}N_4O_6P$ ($[M - CF_3CO_2]^+$) 711.3311, $C_{40}H_{49}N_4O_6P$ ($[M - CF_3CO_2 + H]^{2+}$) 356.1689. Found: 711.3320, 356.1727.

DO3A-xy-TTP trifluoroacetate. Following **general procedure 3**, the title compound was prepared from **3b** (0.21 g, 0.23 mmol) and trifluoroacetic acid (2.1 mL) as a white solid (0.10 g, 57%). ^{1}H-NMR (400 MHz, MeOD) δ_H (ppm): 7.58–7.52 (12H, m, *o*/*m*-Ar), 7.47 (2H, d, $^3J_{HH}$ = 8.2 Hz, $C_6\underline{H}_4$), 7.09 (2H, broad s, $C_6\underline{H}_4$), 4.83 (2H, d, $^2J_{HP}$ = 15.3 Hz, $C\underline{H}_2P$), 4.48 (2H, broad s), 4.15 (2H, broad s), 3.78–3.43 (4H, m, $C\underline{H}_2CO_2H$), 3.29–2.90 (16H, m, macrocycle $\underline{H}$). 2.50 (9H, s, $C\underline{H}_3$). $^{13}C\{^1H\}$-NMR (100 MHz, MeOD) δ_C (ppm): 174.2 ($\underline{C}$═O), 171.7 ($\underline{C}$═O), 148.2 (*p*-Ar), 135.2 (d, $^3J_{CP}$ = 10.3 Hz, $\underline{C}_6H_4$), 133.2 (d, $^4J_{CP}$ = 5.4 Hz, $\underline{C}_6H_4$), 132.0 (d, $^2J_{CP}$ = 12.4 Hz, *o*-Ar), 121.9 ($\underline{C}_6H_4$), 119.0 (*m*-Ar), 115.7 (d, $^1J_{CP}$ = 90.2 Hz, *i*-Ar), 113.2 ($\underline{C}_6H_4$), 58.6, 55.4, 53.6 ($\underline{C}H_2CO_2H$), 50.8 (broad, macrocycle $\underline{C}$), 30.7 (d, $^1J_{CP}$ = 48.7 Hz, $\underline{C}H_2P$), 21.8 ($\underline{C}H_3$). $^{19}F\{^1H\}$-NMR (377 MHz, MeOD) δ_F (ppm): −77.3. $^{31}P\{^1H\}$-NMR (162 MHz, MeOD) δ_P (ppm): 22.0. HRMS (ES-TOF+): *m*/*z* calcd for $C_{43}H_{54}N_4O_6P$ ($[M - CF_3CO_2]^+$) 753.3781, $C_{43}H_{55}N_4O_6P$ ($[M - CF_3CO_2 + H]^{2+}$) 377.1924. Found: 753.3786, 377.2102.

DO3A-xy-TXP trifluoroacetate. Following **general procedure 3**, the title compound was prepared from **3c** (0.33 g, 0.32 mmol) and trifluoroacetic acid (3.3 mL) as a white solid (0.17 g, 57%). ^{1}H NMR (400 MHz, MeOD) δ_H (ppm): 7.52 (3H, s, *p*-Ar), 7.49 (2H, d, $^3J_{HH}$ = 7.7 Hz, $C_6\underline{H}_4$), 7.18 (6H, d, $^3J_{HP}$ = 13.1 Hz, *o*-Ar), 7.00 (2H, d, $^3J_{HH}$ = 6.7 Hz, $C_6\underline{H}_4$), 4.68 (2H, d, $^2J_{HP}$ = 15.0 Hz, $C\underline{H}_2P$), 4.24 (2H, s), 3.83 (2H, s), 3.64 (2H, s), 3.42–3.01 (18H, m, macrocycle $\underline{H}$), 2.36 (18H, s, $C\underline{H}_3$). $^{13}C\{^1H\}$-NMR (100 MHz, MeOD) δ_C (ppm): 161.6 ($\underline{C}$═O), 161.3 ($\underline{C}$═O), 140.4 (d, $^2J_{CP}$ = 13.7 Hz, $\underline{C}_6H_4$), 136.6 (d, $^4J_{CP}$ = 3.7 Hz, *p*-Ar), 132.0 (d, $^4J_{CP}$ = 5.5 Hz, $\underline{C}_6H_4$), 131.5 ($\underline{C}_6H_4$), 131.2 (d, $^2J_{CP}$ = 10.4 Hz, *o*-Ar), 118.3 ($\underline{C}_6H_4$), 117.5 (d, $^1J_{CP}$ = 84.7 Hz, *i*-Ar), 115.4 (*m*-Ar), 56.8, 54.4, 49.8 (broad s), 49.1 (broad s), 48.7 (broad s), 29.2 (d, $^1J_{CP}$ = 49.7 Hz, $\underline{C}H_2P$), 19.9 ($\underline{C}H_3$). $^{19}F\{^1H\}$-NMR (377 MHz, MeOD) δ_F (ppm): −72.6. $^{31}P\{^1H\}$-NMR (162 MHz, MeOD) δ_P (ppm): 22.3. HRMS (ES-TOF+): *m*/*z* calcd for $C_{46}H_{60}N_4O_6P$ ($[M - CF_3CO_2]^+$) 795.4250, $C_{46}H_{61}N_4OP$ ($[M - CF_3CO_2 + H]^{2+}$) 398.2159. Found: 795.4326, 398.2164.

Radiochemistry procedures

General synthesis of [^{68}Ga]Ga-DO3A-xy-TAP. The methodology was a modification of the procedure described by Wang *et al.*[28] To a solution of DO3A-xy-TAP trifluoroacetate (approx. 100 μg) in NH_4OAc buffer (0.1 M, 0.5 mL), an aliquot of [^{68}Ga]$GaCl_3$ in 0.1 M HCl (approx. 150 MBq, 0.5 mL) was added, and the resulting mixture was heated at 100 °C for 30 min to yield the desired product. Initial QC was performed using iTLC and a mobile phase of 0.1 M disodium EDTA and by the analytical HPLC method described previously.

Determination of Log *D* values. As an index for lipophilicity, octanol/phosphate buffered saline (PBS) partition coefficient (log *D*) values of the [^{68}Ga]Ga-DO3A-xy-TAP compounds were determined. A general methodology is as follows: aliquots of the radiolabelled compound (10 μL, ∼4 kBq) were added to vials containing a layered mixture of *n*-octanol (500 μL) and PBS solution (pH 7.4, 500 μL). After vortex mixing for 1 min, the mixture was centrifuged to separate the octanol–PBS phases (10^4 rpm, 2 min), before aliquots of the two phases (100 μL) were taken, and transferred into vials for counting. Relative amounts of test compound in each phase were determined by an automatic gamma counter. The log *D* value was reported as the average of data obtained in 6 independent experiments.

In vitro tumour uptake study

For the tumour uptake study, MDA-MB 231 breast cancer cells were used. [^{68}Ga]Ga-DO3A-xy-TXP and [^{68}Ga]Ga(III) were dissolved in serum-free cell medium to give a concentration of 1 MBq mL^{-1}. 100 kBq aliquots of radiotracer were added to cell samples (2 mL, 5 × 10^5 cells per mL) and incubated for 30 min. The cell supernatant was transferred to tubes for gamma counting, before the cells were washed with PBS which was subsequently added to the cell supernatant. The cells were harvested by addition of trypsin (300 μL) and washing with a

serum-free cell medium (700 μL). The supernatant and the harvested cells were assayed in an automatic gamma counter to determine percentage tracer uptake. The experiments were performed in triplicate.

Langendorff isolated heart perfusion

Animals. Male Wistar rats (240–275 g; Charles River Laboratories) were used for all experiments. Animal procedures were in accordance with the Animals (Scientific Procedures) Act, UK, 1986.

The triple-γ-detector system. We developed a system for characterizing the pharmacokinetics of radionuclide passage through an isolated perfused heart comprising 3 orthogonally orientated lead-collimated Na/I γ detectors positioned: (i) 3 cm downstream of a radiotracer injection port on the arterial line, 15 cm upstream of the heart cannula (to provide a radiotracer input function); (ii) directly opposite the heart itself; and (iii) over the venous outflow line (to provide an output function). Each was connected to a modified GinaSTAR instant thin-layer chromatography system running Gina software (Raytest Ltd).

Experimental protocol. Rats were anaesthetized with sodium pentobarbital and heparin sodium (200 mg kg^{-1} and 200 IU kg^{-1} respectively, i.p.) and their hearts were excised and cannulated in the Langendorff mode as previously described.[51] The hearts were perfused at 14 mL min^{-1} constant flow with modified Krebs–Henseleit buffer (mKHB) containing NaCl (118 mM), KCl (5.9 mM), $MgSO_4$ (2.3 mM), $NaHCO_3$ (25 mM), EDTA (0.65 mM), glucose (11.1 mM) and $CaCl_2$ (2.5 mM). The mKHB was freshly prepared and filtered before use, and was gassed with 95% O_2 and 5% CO_2 and used at 37 °C. A left ventricular balloon was used to measure contractile function.

After a 10 min stabilization period, a bolus of radiotracer (1 MBq) was injected into the arterial line, and the activity at the arterial, heart and venous detectors was recorded (Fig. 4A). After 15 minutes, a 6 μM solution of CCCP in mKHB heated to 37 °C was infused *via* the arterial line at 1.4 mL min^{-1}, whilst the flow rate at the peristaltic pump was reduced by 10%. A further 1 MBq radiotracer bolus was administered 5 minutes after the commencement of CCCP infusion. The radiotracer retained after 15 min in both the healthy and CCCP-infused hearts was reported as the average of the normalized activity between 14–15 minutes after the radiotracer injection.

Author contributions

N.L. and R.S. jointly supervised the work. A.S. carried out the synthetic chemistry, radiochemistry and isolated heart perfusion. P.G. carried out the cell work. A.S., N.L., R.S., P.B. and M.M. co-authored the manuscript.

Conflicts of interest

There are no conflicts to declare.

Acknowledgements

We would like to thank the KCL/ICL EPSRC CDT in Medical Imaging (grant EP/L015226/1) for providing funding for A. S. and P. G. This research was supported by the Centre of Excellence in Medical Engineering funded by the Wellcome Trust and EPSRC (203148/Z/16/Z).

Notes and references

1 M. P. Murphy, *Trends Biotechnol.*, 1997, **15**, 326–330.
2 M. P. Murphy, *Biochim. Biophys. Acta, Bioenerg.*, 2008, **1777**, 1028–1031.
3 D.-Y. Kim and J.-J. Min, *Nucl. Med. Mol. Imaging*, 2016, **50**, 185–195.
4 J. Zielonka, J. Joseph, A. Sikora, M. Hardy, O. Ouari, J. Vasquez-Vivar, G. Cheng, M. Lopez and B. Kalyanaraman, *Chem. Rev.*, 2017, **117**, 10043–10120.
5 B. Kadenbach, R. Ramzan, R. Moosdorf and S. Vogt, *Mitochondrion*, 2011, **11**, 700–706.
6 B. Zhang, D. Wang, F. Guo and C. Xuan, *Fam. Cancer*, 2015, **14**, 19–23.
7 R. C. Scaduto and L. W. Grotyohann, *Biophys. J.*, 1999, **76**, 469–477.
8 S. Nigam, B. P. Burke, L. H. Davies, J. Domarkas, J. F. Wallis, P. G. Waddell, J. S. Waby, D. M. Benoit, A. M. Seymour, C. Cawthorne, L. J. Higham and S. J. Archibald, *Chem. Commun.*, 2016, **52**, 7114–7117.
9 A. Baracca, G. Sgarbi, G. Solaini and G. Lenaz, *Biochim. Biophys. Acta, Bioenerg.*, 2003, **1606**, 137–146.
10 J. Maddahi, H. Kiat, K. F. Van Train, F. Prigent, J. Friedman, E. V. Garcia, N. Alazraki, E. G. DePuey, K. Nichols and D. S. Berman, *Am. J. Cardiol.*, 1990, **66**, 55E–62E.
11 J. D. Kelly, A. M. Forster, B. Higley, C. M. Archer, F. S. Booker, L. R. Canning, K. W. Chiu, B. Edwards, H. K. Gill and M. McPartlin, *J. Nucl. Med.*, 1993, **34**, 222–227.
12 M. L. Chiu, J. F. Kronauge and D. Piwnica-Worms, *J. Nucl. Med.*, 1990, **31**, 1646–1653.
13 D. Piwnica-Worms, J. F. Kronauge and M. L. Chiu, *Circulation*, 1990, **82**, 1826–1838.
14 Y. Zhou, Y.-S. Kim, X. Yan, O. Jacobson, X. Chen and S. Liu, *Mol. Pharm.*, 2011, **8**, 1198–1208.
15 M. D. Bartholomä, S. Zhang, V. Akurathi, C. A. Pacak, P. Dunning, F. H. Fahey, D. B. Cowan, S. Ted Treves and A. B. Packard, *Nucl. Med. Biol.*, 2015, **42**, 796–803.
16 H. Yuan, H. Cho, H. H. Chen, M. Panagia, D. E. Sosnovik and L. Josephson, *Chem. Commun.*, 2013, **49**, 10361–10363.
17 T. Mou and X. Zhang, *Molecules*, 2017, **22**, 562.
18 M. F. Ross, T. Da Ros, F. H. Blaikie, T. A. Prime, C. M. Porteous, I. I. Severina, V. P. Skulachev, H. G. Kjaergaard, R. A. J. Smith and M. P. Murphy, *Biochem. J.*, 2006, **400**, 199–208.
19 H. Fukuda, A. Syrota, P. Charbonneau, J. Vallois, M. Crouzel, C. Prenant, J. Sastre and C. Crouzel, *Eur. J. Nucl. Med. Mol. Imaging*, 1986, **11**, 478–483.

20 H. T. Ravert, I. Madar and R. F. Dannals, *J. Labelled Compd. Radiopharm.*, 2004, **47**, 469–476.
21 D. Y. Kim, H. J. Kim, K. H. Yu and J. J. Min, *Bioconjugate Chem.*, 2012, **23**, 431–437.
22 D.-Y. Kim, H.-J. Kim, K.-H. Yu and J.-J. Min, *Bioorg. Med. Chem. Lett.*, 2012, **22**, 319–322.
23 G. Zhao, Y. M. Yu, T. M. Shoup, D. R. Elmaleh, A. A. Bonab, R. G. Tompkins and A. J. Fischman, *J. Surg. Res.*, 2014, **188**, 473–479.
24 Z. Zhao, Q. Yu, T. Mou, C. Liu, W. Yang, W. Fang, C. Peng, J. Lu, Y. Liu and X. Zhang, *Mol. Pharm.*, 2014, **11**, 3823–3831.
25 T. Tominaga, H. Ito, Y. Ishikawa, R. Iwata, K. Ishiwata and S. Furumoto, *J. Labelled Compd. Radiopharm.*, 2016, **59**, 117–123.
26 A. Haslop, A. Gee, C. Plisson and N. Long, *J. Labelled Compd. Radiopharm.*, 2013, **56**, 313–316.
27 A. Haslop, L. Wells, A. Gee, C. Plisson and N. Long, *Mol. Pharm.*, 2014, **11**, 3818–3822.
28 J. Wang, C. T. Yang, Y. S. Kim, S. G. Sreerama, Q. Cao, Z. B. Li, Z. He, X. Chen and S. Liu, *J. Med. Chem.*, 2007, **50**, 5057–5069.
29 C.-T. Yang, Y. Li and S. Liu, *Inorg. Chem.*, 2007, **46**, 8988–8997.
30 Y. Zhou and S. Liu, *Bioconjugate Chem.*, 2011, **22**, 1459–1472.
31 F. Roesch, *Curr. Radiopharm.*, 2012, **5**, 202–211.
32 F. Rösch, *Appl. Radiat. Isot.*, 2013, **76**, 24–30.
33 S. R. Banerjee and M. G. Pomper, *Appl. Radiat. Isot.*, 2013, **76**, 2–13.
34 P. Spang, C. Herrmann and F. Roesch, *Semin. Nucl. Med.*, 2016, **46**, 373–394.
35 B. W. Tsang, C. J. Mathias and M. A. Green, *J. Nucl. Med.*, 1993, **34**, 1127–1131.
36 V. Sharma, J. Sivapackiam, S. E. Harpstrite, J. L. Prior, H. Gu, N. P. Rath and D. Piwnica-Worms, *PLoS One*, 2014, **9**, e109361.
37 M. Kardashinsky, N. Lengkeek and L. M. Rendina, *J. Labelled Compd. Radiopharm.*, 2017, **60**, 4–11.
38 E. Mariotti, M. Veronese, J. T. Dunn, R. A. Medina, P. J. Blower, R. Southworth and T. R. Eykyn, *EJNMMI Res.*, 2013, **3**, 74.
39 M. G. Handley, R. A. Medina, E. Mariotti, G. D. Kenny, K. P. Shaw, R. Yan, T. R. Eykyn, P. J. Blower and R. Southworth, *J. Nucl. Med.*, 2014, **55**, 488–494.
40 F. Shaughnessy, E. Mariotti, K. P. Shaw, T. R. Eykyn, P. J. Blower, R. Siow and R. Southworth, *EJNMMI Res.*, 2014, **4**, 1–10.
41 R. A. Medina, E. Mariotti, D. Pavlovic, K. P. Shaw, T. R. Eykyn, P. J. Blower and R. Southworth, *J. Nucl. Med.*, 2015, **56**, 921–926.
42 B. Jagadish, G. L. Brickert-Albrecht, G. S. Nichol, E. A. Mash and N. Raghunand, *Tetrahedron Lett.*, 2011, **52**, 2058–2061.
43 R. L. Gallo, J. N. Finkelstein and R. H. Notter, *Biochim. Biophys. Acta*, 1984, **771**, 217–227.
44 Z. M. Saffee, F. Baark, E. Waters, M. Veronese, V. R. Pell, J. E. Clark, L. Livieratos, T. R. Eykyn, P. J. Blower and R. Southworth, *Sci. Rep.*, 2018, accepted.
45 Y.-S. Kim, Z. He, W.-Y. Hsieh and S. Liu, *Bioconjugate Chem.*, 2007, **18**, 929–936.
46 S. E. Abu-Gosh, N. Kolvazon, B. Tirosh, I. Ringel and E. Yavin, *Mol. Pharm.*, 2009, **6**, 1138–1144.
47 L. B. Chen, *Annu. Rev. Cell Biol.*, 1988, **4**, 155–181.
48 G. Kroemer and J. Pouyssegur, *Cancer Cell*, 2008, **13**, 472–482.
49 D. M. Hockenbery, *Cancer Cell*, 2002, **2**, 1–2.
50 F. G. Mann and E. J. Chaplin, *J. Chem. Soc.*, 1937, 527–535.
51 R. Southworth and P. B. Garlick, *Am. J. Physiol.: Heart Circ. Physiol.*, 2003, **285**, H316–H324.

